Elastomeric Polypropylenes from Unbridged (2-Phenylindene)zirconocene Catalysts: Thermal Characterization and Mechanical Properties

Yirong Hu,[†] Mark T. Krejchi,[†,§] Chirag D. Shah,[†] Charles L. Myers,[‡] and Robert M. Waymouth*[,†]

Department of Chemistry, Stanford University, Stanford, California 94305, and Research Center, Amoco Chemical Company, Naperville, Illinois 60566

Received March 13, 1998; Revised Manuscript Received July 21, 1998

ABSTRACT: The properties of three elastomeric stereoblock polypropylene (PP) samples made with unbridged 2-phenylindene zirconocene catalysts were investigated. One of the characteristics of these catalysts is the ability to control the structure and properties of the polypropylenes by manipulation of the reaction conditions. Samples PP1 and PP2 were prepared to have similar tacticities (as indicated by IR and NMR spectroscopy) yet different molecular weights. The molecular weight of PP2 is approximately half the molecular weight of PP1. Sample PP3 has a molecular weight similar that of PP2 but is lower in isotactic pentad content. All three samples were separated into fractions that differ in their solubilities in boiling ether and heptane. The fractionation appeared to be governed by tacticity and molecular weight. Thermal analysis by differential scanning calorimetry showed very broad melting endotherms. The broadness of the transitions and the relatively large standard deviations calculated for the enthalpy of fusion are indicative of a multiphase material. X-ray powder diffraction patterns of the three samples and their fractions (except the ether-soluble fractions) all showed characteristic peaks of the α crystalline phase. The heptane-insoluble fractions of both PP1 and PP2 also exhibited γ-phase reflection, whereas in the heptane-soluble fractions, that reflection is less evident. Tensile tests performed on PP1 and PP2 yielded a similar tensile modulus for the two, indicating similar degrees of crystallinity. PP1 exhibited better recovery properties, as measured in tests at 100% and 300% elongation.

Introduction

Semicrystalline polypropylene is a thermoplastic that is widely used due to its excellent properties and low cost. The crystallinity of this material is the consequence of an isotactic microstructure consisting of stereocenters of identical configuration along the polymer backbone. Elastomeric polypropylenes are also known; Natta[1−3] was the first to isolate elastomeric forms of polypropylene and interpret the properties of this material in terms of a stereoblock microstructure consisting of alternating blocks of crystalline isotactic stereosequences and amorphous atactic stereosequences. Since the pioneering efforts of Natta et al., there have been a number of reports of related materials produced by different catalysts,[4] with notable advances by Collette,[5−7] Chien,[8−14] and Collins.[15−17] Recently, we reported another strategy for synthesizing elastomeric polypropylenes by use of a catalyst whose structure was designed to switch between isospecific and aspecific configurations to produce an isotactic/atactic stereoblock homopolymer of propylene.[18−22]

The elastomeric polypropylene isolated by Natta[1−3] was the heptane-soluble fraction of a heterogeneous mixture of polymers produced by a Ziegler-type catalyst, whereas the elastomer synthesized at Dupont[5−7] did not require fractionation to exhibit good elastomeric properties. The Dupont elastomer was heterogeneous in composition and could be separated into several fractions by solvent extraction. A high-molecular-weight, ether-soluble fraction was found to be a critical component of the material—blending of the ether-soluble fraction with isotactic polypropylene yielded a blend that had elastomeric properties quite similar to the unfractionated polymer.[6] In contrast, elastomeric polypropylenes made with stereorigid metallocenes by Chien[8,9,11,14] and Collins[15−17] are much more homogeneous in their composition, being completely soluble in boiling ether.

In this paper, we report the characterization of three samples of elastomeric polypropylene made with unbridged 2-phenylindene zirconocene catalysts. One of the characteristics of these catalysts is the ability to control the structure and properties of the polypropylenes by manipulation of the reaction conditions.[19] Three samples were prepared that differ in molecular weight and tacticity; these were investigated by IR and NMR spectroscopy, gel permeation chromatography

Table 1. Tacticity and Molecular Weight

sample	% wt	fraction	IR index[a]	mmmm[b]	M_w[c] ($\times 10^{-3}$)	M_w/M_n
PP1	100	whole	0.33	0.32	455	2.7
PP1-ES	36	ether	0.19	0.18	339	2.5
PP1-HS	43	heptane	0.33	0.33	367	2.4
PP1-HI	21	insol	0.68	0.51	598	3.1
PP2	100	whole	0.34	0.34	257	3.2
PP2-ES	72	ether	0.19	0.23	192	2.5
PP2-HS	13	heptane	0.52	0.53	263	2.9
PP2-HI	15	insol	1.00	0.81	512	3.0
PP3	100	whole	0.25	0.17	198	3.0
PP3-ES	80	ether	0.17	0.14	174	2.6
PP3-HS	20	heptane	0.42	0.30	244	2.6

[a] Determined by the ratio of absorbance intensity A_{998}/A_{975}. [b] Determined by ^{13}C NMR, the fraction of five contiguous isotactic stereosequences in the polymer. [c] Determined by GPC (waters 150C) at Amoco Chemical Co.

[†] Stanford University.
[§] Present address: Wilsonart International, 505 South General Bruce Drive, Temple, TX 76503.
[‡] Amoco Chemical Co.

S0024-9297(98)00399-4 CCC: $15.00
Published on Web 09/10/1998

Table 2. Pentad Distributions and Statistical Analysis Results

	PP1				PP2				PP3		
	whole	ES	HS	HI	whole	ES	HS	HI	whole	ES	HS
[mmmm]	0.324	0.179	0.331	0.510	0.343	0.227	0.529	0.808	0.168	0.143	0.299
[mmmr]	0.147	0.157	0.159	0.126	0.144	0.168	0.125	0.065	0.164	0.157	0.144
[rmmr]	0.043	0.059	0.045	0.030	0.041	0.053	0.023	0.007	0.060	0.062	0.040
[mmrr]	0.098	0.118	0.108	0.071	0.093	0.121	0.088	0.039	0.118	0.123	0.098
[rmrr] + [mmrm]	0.180	0.216	0.173	0.126	0.158	0.197	0.110	0.044	0.227	0.227	0.153
[mrmr]	0.085	0.113	0.077	0.061	0.082	0.090	0.047	0.013	0.111	0.120	0.096
[rrrr]	0.023	0.032	0.020	0.010	0.024	0.029	0.008	0.001	0.028	0.031	0.030
[mrrr]	0.052	0.075	0.045	0.035	0.058	0.056	0.026	0.005	0.076	0.086	0.070
[mrrm]	0.049	0.051	0.043	0.035	0.058	0.057	0.044	0.019	0.050	0.053	0.070
RSS[a]	0.001	0.003	0.005	0.002	0.004	0.004	0.348	0.043	0.002	0.005	0.010
α[b]	0.964	0.958	0.949	0.981	0.953	0.884	0.954	0.983	0.973	0.616	0.932
σ[c]	0.601	0.577	0.622	0.636	0.579	0.600	0.647	0.751	0.589	0.633	0.548
ω[d]	0.275	0.099	0.296	0.463	0.343	0.241	0.547	0.817	0.064	0.392	0.346

[a] RSS = residual sum of squares $(\sum(I_o - I_c)^2/(I_o + I_c)$ where I_o = observed intensity, I_c = calculated intensity). [b] α is the probability of the selection of a d configuration at a d-preferring site in the enantiomorphic site model. [c] σ is the probability of the selection of an m configuration in the Bernoullian model. [d] ω is the mole fraction of the polymer produced according to the enantiomorphic site model.

Table 3. Mechanical Properties

sample	PP1	PP2
density (g/cm$^{3)}$	0.8690	0.8694
tensile strength (MPa)	9.31 (s_d[d] = 0.99)	6.95 (s_d = 0.73)
elongation to break (%)	878 (s_d = 74)	753 (s_d = 116)
tensile modulus (MPa)	13.45 (s_d = 0.73)	15.98 (s_d = 2.07)
tensile stress relaxation (%)[a]	54	67
set (%)[b]	30−40	50−90
hysteresis test[c]		
set after 1st cycle (%) cumulative set after 1st and 2nd cycles (%)	8	16
	12	18
stress relaxation 1st cycle, 30 s (%)	42	49
stress relaxation 2nd cycle, 30 s (%)	29	37
stress relaxation 3rd cycle, 30 s (%)	27	36
retained force, 50% recovery, 2nd cycle (%)	23	6

[a] 50% strain, 5 min. [b] After recovery from 300% elongation, no hold at extension. [c] Three extension cycles to 100% elongation, 30 s hold at extension, 60 s at recovery. [d] Standard deviation.

(GPC), differential scanning calorimetry (DSC), X-ray powder diffraction, and tensile and recovery tests.

Results

The elastomeric polypropylenes investigated in this study were produced in a 2-gallon reactor with the unbridged metallocene bis(2-phenylindenyl)zirconium dichloride/MAO. Sample PP1 was prepared in liquid propylene at 23 °C, sample PP2 was prepared similarly except that hydrogen (0.044 mmol/mol of C_3) was added to reduce the molecular weight. Sample PP3 was prepared in hexane solution at 50 psig propylene pressure.

As shown in Tables 1 and 2,[23] samples PP1 and PP2 have similar tacticities, as indicated both by the isotactic pentad content [mmmm] ([PP1, [mmmm] = 0.32; PP2, [mmmm] = 0.34; determined by ^{13}C NMR) and by the IR index[24,25] (=A_{998}/A_{975}) which is a measure of the isotactic helix content. The molecular weight of PP2 is approximately half the molecular weight of PP1. Sample PP3 has a molecular weight similar to that of PP2 (M_w = 200 000 vs 250 000) but is lower in isotactic pentad content. The molecular weight distributions for the three samples are in the range M_w/M_n = 2.4−3.2.

Mechanical Tests. Tensile tests and recovery tests were performed on samples PP1 and PP2 (Table 3). The density and tensile modulus of the two materials are about the same, indicating similar degrees of crystallinity. The tensile modulus of PP2 is slightly higher than that of PP1 (Figure 1a). Neither polymer exhibits a yield stress maximum. These tensile stress/strain plots are representative of elastomeric polypropylene samples from the same family of catalysts that have been previously tested and that are in the same density or modulus range.[26]

Relative to PP2, PP1 exhibits a higher ultimate tensile strength and a higher slope of stress/strain at high elongations, and it also has better recovery properties, as measured in tests at 100% and 300% elongation. After recovery from 300% elongation, the set (increase in specimen gauge length after recovery) for PP1 is 30−40%, whereas that for PP2 is 50−90% (Figure 1b). For the 100% elongation hysteresis test (Figure 1c), the specimen was elongated to twice its original length in three successive cycles of extension and recovery, with a 30 s hold at 100% elongation and a 60 s hold after recovery between the cycles. The cumulative set after first and second cycles was 12% for PP1 and 18% for PP2. During the 30 s hold in the second cycle, PP1 showed a stress relaxation (decay in stress while held at extension) of 29%, which was 8% less than that for PP2. The retained force (recovery force at an arbitrary point during recovery, relative to extension force) measured in the same cycle at the point of 50% recovery was 23% for PP1 and only 6% for PP2.

Fractionation. All three samples, PP1, PP2, and PP3 can be separated into fractions that differ in their solubilities in boiling ether and heptane (Table 1). Samples PP1 and PP2 yielded ether-soluble (ES), heptane-soluble (HS), and heptane-insoluble (HI) fractions, while sample PP3 yielded only ether- and heptane-soluble fractions. Fractionation appears to be governed

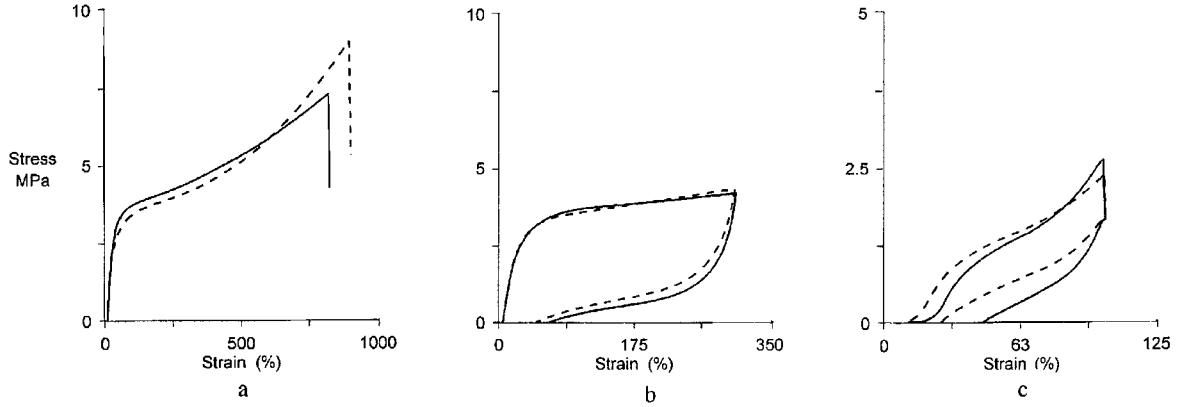

Figure 1. (a) Tensile test for PP1 and PP2. (b) 300% elongation recovery test for PP1 and PP2. (c) 100% elongation hysteresis test for PP1 and PP2, second cycle.

by tacticity and molecular weight—samples with higher isotactic pentad contents and molecular weights are less soluble. The isotactic pentad contents of the fractions span a considerable range and vary from $0.14 \leq [mmmm] \leq 0.81$.

Despite the similar tacticities for the raw polymers, PP1 and PP2 fractionate differently. PP1 yields only 36% of an ether-soluble fraction, while 72% of PP2 is soluble in ether. Both ES fractions have similar tacticities. The heptane-soluble fraction of PP1 (43%) has a similar isotactic pentad content to the whole polymer ([mmmm] = 0.33) while PP2−HS is a smaller fraction of PP2 (13%), but has a higher isotactic pentad content ([mmmm] = 0.53). The heptane-insoluble fraction of PP2 is quite high in isotactic pentad content with [mmmm] = 0.81.

The molecular weights of the various fractions of PP3 are similar. For PP1 and PP2, the HI fraction has the highest molecular weight. The molecular weight distributions for all of the fractions vary slightly and fall in the range $2.4 \leq M_w/M_n \leq 3.2$.

Thermal Analysis. Thermal analysis of the polypropylene samples and their fractions was carried out by differential scanning calorimetry. All samples were pretreated to 200 °C to provide a consistent thermal history. The temperatures and enthalpies of crystallization were obtained by cooling samples from +200 to −25 °C at 20 °C/min. Melting temperatures and enthalpies of fusion were obtained in two ways. In the first case, samples were cooled quickly from +200 to −50 °C at 200 °C/min and then reheated to 200 °C at 20 °C/min. Aged samples were prepared by allowing the samples cooled from 200 °C to sit at room temperature for 20 h prior to the heating run.

Cooling studies gave the most reproducible results and revealed reasonably sharp crystallization exotherms. The heating curves display very broad melting endotherms with the onset of melting appearing at or below room temperature and continuing up to a peak ranging from 80 to 142 °C. Typical heating and cooling curves are shown in Figure 2.

The thermal properties of the polypropylene samples are reported in Table 4. Melting points are reported as the peak of the melting endotherms. The broad melting endotherms made determination of the enthalpies of fusion difficult; averages of several runs (with standard deviations) are reported.

For all samples, the enthalpies of crystallization measured during cooling are lower than the enthalpies of fusion measured during the heating runs. Enthalpies

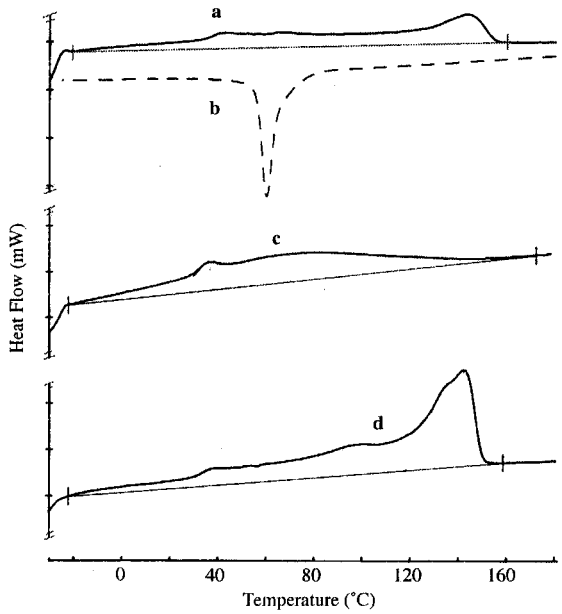

Figure 2. (a) Heating and (b) cooling curve for PP1. (c) Heating curve for PP1-HS. (d) Heating curve for PP1-HI.

of fusion also increase upon aging the samples for 20 h at room temperature, particularly for samples of higher crystallinity.

Samples PP1 and PP2 exhibit similar crystallization and melting temperatures ($T_c \approx 60$ °C, $T_m \approx 140$ °C), but the degree of crystallinity appears slightly higher for PP2, as indicated in the higher enthalpy of fusion ($\Delta H_f = 24$ ($s_d = 2.5$) vs 36.7 ($s_d = 0.3$)). The isotactic pentad content of PP3 is considerably lower than that of PP1 and PP2 ([mmmm] = 0.17 vs [mmmm] = 0.30), yet the peak melting point is only 10 °C lower at $T_m \approx$ 130 °C. The crystallization temperatures and enthalpies of crystallization/fusion are much lower for PP3 compared to PP1 and PP2, as expected for a sample of lower isotactic pentad content.

The ether-soluble fractions show no thermal transitions under these experimental conditions. For the other fractions, the crystallization/melting temperatures and enthalpies of crystallization/fusion increase with increasing isotactic pentad content.

X-ray powder diffraction patterns were taken on pressed polymer films that had been heated to 200 °C, cooled slowly to room temperature, and allowed to sit overnight prior to analysis. Representative 2θ scans are given in Figures 3 and 4.

Table 4. Thermal Properties

sample	mmmm[a]	M_w[b] ($\times 10^{-3}$)	T_c (°C)	ΔH_c (J/g)	T_m (°C)	ΔH_f (J/g)	$s_{d,\Delta H_f}$[c] (J/g)	ΔH_f (aged) (J/g)	$s_{d,\Delta H_{f(aged)}}$[d] (J/g)
PP1	0.32	455	61.1	−12.1	138.1	24	2.8	24	2.5
PP1-ES	0.18	339							
PP1-HS	0.33	367			79.7	11.0	0.9	35	8.0
PP1-HI	0.51	598	85.8	−38.7	141.6	65	6.5	73	4.0
PP2	0.34	257	63.4	−17.0	140.1	31	4.9	36.7	0.3
PP2-ES	0.23	192							
PP2-HS	0.53	263	71.0	−23.2	134.8	57	3.8	71	4.1
PP2-HI	0.81	512	94.1	−67.7	139.8	100	5.8	106	5.9
PP3	0.17	198	29.2	−1.0	131.8	8.1	1.2	17	3.1
PP3-ES	0.14	174							
PP3-HS	0.30	244	51.0	13.5	127.9	45	5.9	51	8.0

[a] Determined by ^{13}C NMR, the fraction of five contiguous isotactic stereosequences in the polymer. [b] Determined by GPC (waters 150C) at Amoco Chemical Co. [c] Standard deviation calculated for ΔH_f. [d] Standard deviation calculated for ΔH_f (aged).

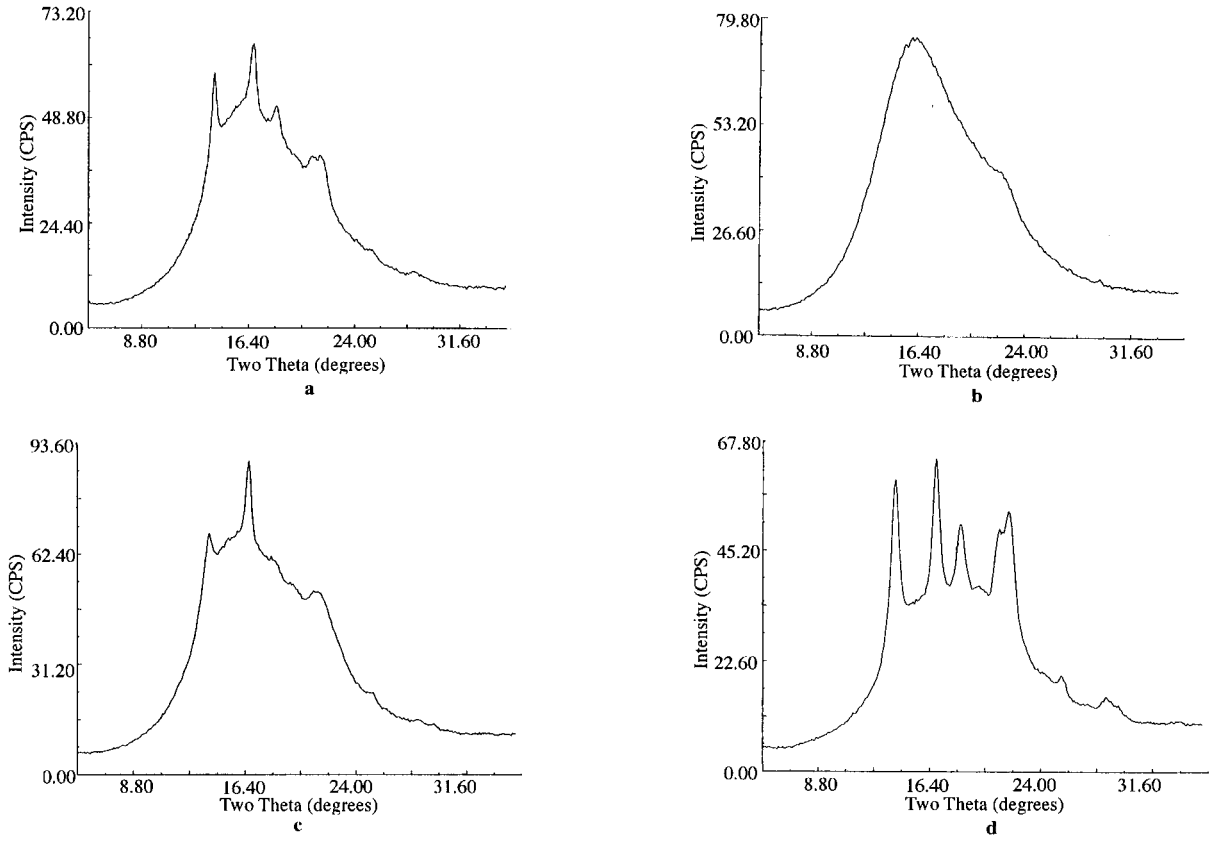

Figure 3. X-ray diffraction patterns (2θ) of (a) PP1, (b) PP1-ES, (c) PP1-HS, and (d) PP1-HI.

Table 5. Crystallinity and Crystalline Form

sample	% crystallinity[a] (from DSC)	% crystallinity (from X-ray)	% α form	% γ form
PP1	11	15	15	0
PP1-ES		smectic		
PP1-HS	17	13	6	7
PP1-HI	35	22	17	5
PP2	18	14	14	0
PP2-ES		smectic		
PP2-HS	34	21	10	11
PP2-HI	51	38	29	9
PP3	8	3	3	0
PP3-ES		smectic		
PP3-HS	24	16	10	6

[a] Since $\Delta H = 209$ J/g for 100% crystalline polypropylene, % crystallinity $= \Delta H_{f(aged)}/209$.

From the diffraction patterns of PP1 and PP2, characteristic reflections at $2\theta = 14.0°$, 16.8°, 18.6°, 21.1°, and 21.7° for the α-phase[27,28] of polypropylene are evident, particularly in the HI fractions. In addition, for PP2-HS and PP2-HI, a characteristic reflection at $2\theta = 20.07°$ for the γ-phase[28,29] of polypropylene is evident.

Deconvolution of the X-ray patterns required two amorphous background peaks at $2\theta =$ approximately 16° and 21° for adequate fitting of the pattern. While this procedure is somewhat arbitrary, it may be indicative of some smectic or β-phase polypropylenes present in these multiphase materials. The patterns were fit to no more than seven α peaks and in some cases one γ peak ($2\theta = 20.07°$) while constraining the two amorphous peaks. The percent crystallinities reported in Table 5 were estimated by taking the ratio of the integrated area under all crystalline peaks to the total area. Calculated values for the percent crystallinity by X-ray are similar to those calculated by DSC for the aged samples (Table 5).

Crude estimates for the percentage of α and γ phases were calculated from the area of the reflection at $2\theta =$ 20.07°. From Brückner and Meille,[30] we obtain the

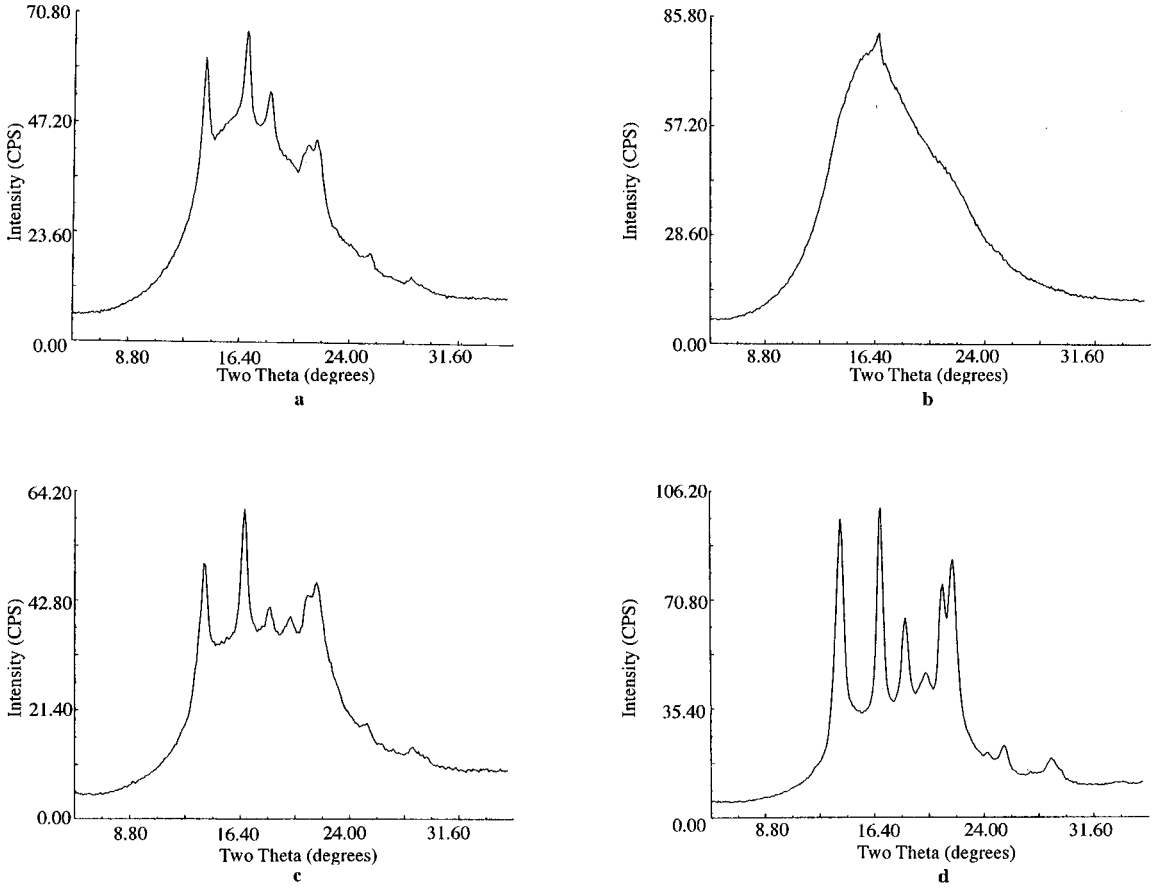

Figure 4. X-ray diffraction patterns (2θ) of (a) PP2, (b) PP2-ES, (c) PP2-HS, and (d) PP2-HI.

ratio: (total area under all γ peaks)/(area under γ peak at $2\theta = 20.07°$) = 4.47.

Multiplication of the area under the peak at $2\theta = 20.07°$ in our fitted pattern by this ratio gives a rough estimate of the total area of all γ peaks. This value was then subtracted from the area under all crystalline peaks to get an estimate of the percentage of α and γ phases in the sample.

As shown in Table 5, all three samples contain the α crystalline phase of polypropylene. The ether-soluble fractions of the three samples are suggestive of the smectic phase, and the other fractions show a mixture of α and γ crystalline phases. Estimates for the percentage of γ-phase range from 5 to 11% in these samples.

Discussion

The elastomeric polypropylenes characterized in this study were synthesized with a metallocene catalyst derived from bis(2-phenylindenyl)zirconium dichloride/MAO. We have previously shown that the microstructure and physical properties of these materials can be manipulated by varying the reaction conditions such as monomer concentration and temperature.[18−22] For this study, three samples were prepared for comparison. PP1 and PP2 have similar tacticities but different molecular weights, whereas PP2 and PP3 have similar molecular weights but different tacticities.

Characterization of these materials was carried out by ^{13}C NMR spectroscopy, IR spectroscopy, differential scanning calorimetry, wide-angle X-ray diffraction, and mechanical testing. The microstructure of the polymer was investigated by ^{13}C NMR and IR. One measure of tacticity is the isotactic pentad content [mmmm], which is the fraction of five contiguous isotactic stereosequences in the polymer. The IR index A_{998}/A_{975} is a related indicator that provides a measure of the isotactic helix content in the polymer. The band at 998 cm^{-1} corresponds to sequence lengths of approximately 10−14 isotactic repeat units in helical conformations, whereas the band at 975 cm^{-1} corresponds to head-to-tail sequences of propylene units.[25,31]

All three samples are low in isotactic pentad content, with [mmmm] between 0.17 and 0.33. Statistical analysis of the pentad distributions of PP1, PP2, and PP3 cannot be modeled well with single-site propagation statistics (Bernoullian, enantiomorphic-site, or Markovian statistical models). The spectra are best fitted by a concurrent two-site model proposed by Zambelli,[32] Chûjô, and co-workers[23,33,34] which describes either a stereoblend or a stereoblock polymer. This model assumes there are two different catalytic sites, one leading to isotactic and the other to atactic stereosequences. The triad and pentad tacticities of the resulting polymer can be described with three parameters. σ is the probability of the selection of an m configuration at an atactic site, α is the probability of the selection of a d configuration at a d-preferring enantiomorphic site, and the third parameter ω is the mole fraction of the polymer produced at the enantiomorphic sites. Thus ω is essentially equal to the isotactic fraction in a stereoblock polymer. Fitting by the concurrent two-site model gives similar isotactic fractions for PP1 and PP2 (PP1, $\omega = 26\%$; PP2, $\omega = 32\%$). These values are approximately twice as high as the degree of crystallinity obtained from DSC and X-ray studies. This is not unreasonable since

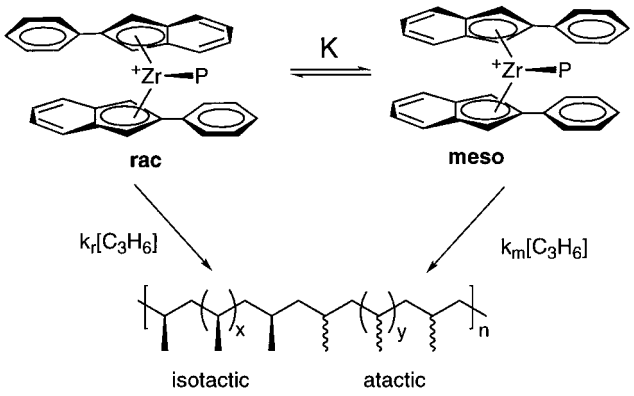

Figure 5. Proposed mechanism for the formation of elastomeric polypropylene.

isotactic polypropylene, for which ω = 100%, is approximately 60% crystalline. The calculated isotactic fraction for PP3 is 5.8%. The difference between its isotactic fraction and degree of crystallinity for this sample is quite small, probably due to its extremely low crystallinity.

PP2 and PP3 are similar in molecular weight (M_w = 250 000 vs 200 000). The molecular weight of PP1 is approximately twice as high. The molecular weight distributions of the three samples fall between 2.7 and 3.2. In comparison, elastomeric polypropylenes produced by Chien[8−14] typically are of lower molecular weights (M_w < 170 000) and narrower molecular weight distributions ($M_w/M_n \approx 2$), while those produced with heterogeneous catalysts by Collette[5−7] have higher molecular weights (M_w = 350 000 and 600 000) and broader molecular weight distributions ($M_w / M_n \geq 5.8$).

Metallocene catalysts typically produce polymers with M_w/M_n = 2.0. A value between 2.7 and 3.2 would suggest that in contrast to most metallocenes, the 2-arylindene catalysts generate several active sites during the polymerization reaction. We have proposed a mechanism that invokes an aspecific site and an isospecific site that interconvert during the construction of a single polymer chain (Figure 5). Each of these catalytic states may be predisposed to give polymers of different molecular weights. As pointed out by Coleman and Fox,[35] when the catalytic states interconvert rapidly (several transitions occur between successive additions of monomer), the molecular weight distribution of the resulting polymer will be narrow. On the other hand, if the states do not interconvert at all, M_w/M_n will be broader and reflect the difference in molecular weights at the various sites. The fact that the molecular weight distributions fall between 2.7 and 3.2 for our polymers could be interpreted as the catalytic states interconverting at an intermediate rate during polymerization. While this mechanism predicts that the molecular weight distribution could be broader than that expected for a single-site catalyst, it is not clear that the magnitude of the molecular weight distribution as well as the fractionation behavior (vida infra) can be completely accounted for by the Coleman and Fox kinetic model.

The mechanical properties of the stereoblock polypropylenes are reported in Table 3. In contrast to highly crystalline polypropylene, the elastomeric polypropylenes exhibit no plastic yield in stress/strain measurements. The elastic properties are further demonstrated in the hysteresis tests where the samples show partial elastic recovery as they are successively cycled to 100% and 300% elongation. PP1 exhibits higher ultimate tensile strength and higher slope in the stress/strain curve at high elongations; this may be related to its higher molecular weight and to differences in stereoblock composition. However, considering the standard deviations in the tests (Table 3) and limited comparisons of data, we would recommend caution in any rationalization of the tensile differences. PP1 also has better recovery properties compared to PP2, a likely consequence of the difference in molecular weight (M_w = 455 000 vs 257 000).

Thermal properties of the polymers were studied by DSC and wide-angle X-ray diffraction. The three samples were all treated in the same way prior to the DSC runs to ensure consistent thermal history. Each run was repeated three times for reproducibility. The cooling studies gave the most reproducible results with a standard deviation <0.2 (J/g) for ΔH_c. The crystallization exotherms are reasonably sharp compared to the melting endotherms in the heating runs. The broadness of the melting peaks and the relative large standard deviations for ΔH_f are indicative of the different crystalline structures that coexist in each sample.

The enthalpy of fusion for each sample is typically more than twice as high as its enthalpy of crystallization. This is likely a consequence of the kinetics of crystallization. Also, all the samples show an increase in ΔH_f after aging, accompanied by double melting peaks with the first peak around 35−40 °C and the second peak around 135−140 °C. Samples PP1 and PP2 have similar T_c's and T_m's. For sample PP3, its crystallization temperature and enthalpies of crystallization/fusion are much lower. As shown in Table 4, ΔH_c for PP3 is less than one-tenth of that for PP1 or PP2, despite the fact that the isotactic pentad contents of PP1 and PP2 are only twice as high. This indicates the differences in their stereosequence distribution or isotactic sequence lengths. Among the three samples, PP2 has the highest degree of crystallinity, as indicated by ΔH_f.[36]

X-ray powder diffraction patterns of samples PP1, PP2, and their fractions, shown in Figure 3 and Figure 4, show the five characteristic α peaks[27,28] in all patterns except ether-soluble fractions. The HI fractions of both PP1 and PP2 clearly showed γ reflection[28,29] at 2θ = 20.07°, whereas in the HS fractions that reflection is less evident. Efforts to deconvolute the ES powder patterns were not successful as a result of their highly amorphous nature.

The degree of crystallinity estimated from DSC studies are higher than those calculated from X-ray data analysis, particularly for samples with higher crystallinity (Table 5). This is probably due to the fact that the degree of crystallinity calculated from the area under the crystalline peaks in the X-ray diffraction patterns only took into consideration contributions from the α and γ crystalline phases and neglected the possible contribution from other less ordered phases such as the β-phase. Collette[5−7] reported that elastomeric polypropylenes prepared with heterogeneous zirconium alkyls on alumina could be separated into three fractions by successive extraction with boiling ether and heptane. In one case, a heptane-insoluble fraction of M_w greater than 2 500 000 was obtained. The molecular weight distributions of the ether-soluble fraction and the heptane-insoluble fraction are close to that of the whole

polymer. The heptane-soluble fraction, however, has a very broad molecular weight distribution (>20). In contrast, elastomeric polypropylenes produced by Chien[8,9,11,14] are quite homogeneous, being completely soluble in refluxing ether and having molecular weight distributions less than 2.

Fractionation of PP1 and PP2 each yielded three fractions that differ in tacticity. As indicated by IR and ^{13}C NMR, the ether-soluble fractions have the lowest isotactic pentad contents and the heptane-insoluble fractions the highest. PP3 only yielded two fractions, the ether-soluble fraction and the heptane-soluble fraction, with the latter higher in isotactic pentad content. In both PP1 and PP2, the heptane-insoluble fraction has the highest molecular weight. The fractions of PP3 are all similar in molecular weight. The fact that samples with higher isotactic pentad contents are less soluble suggests that a sample's solubility is determined by its crystallinity; however, molecular weight also appears to play a role.

A comparison between the fractions of PP1 and those of PP2 revealed some surprising features. Addition of hydrogen during polymerization causes a decrease in molecular weight for PP2 and its ether-soluble and heptane-soluble fractions. ES fractions of PP1 and PP2 have similar isotactic pentad contents (0.18 vs 0.23), yet the weight percentage of ES fraction produced is much higher in the presence of hydrogen (72% vs 36%). In addition, a comparison between the HI fractions of PP1 and PP2 showed that the weight percentage and the molecular weight of the HI fraction are not significantly influenced by the addition of hydrogen, yet the isotactic pentad content of the HI fraction in PP2 ([mmmm] = 0.81) is higher than that in PP1 ([mmmm] = 0.51). The origin of this behavior is not clear. There have been reports in the literature that the productivity and stereospecificity of metallocene catalysts can increase in the presence of hydrogen.[37] Thus it is possible that the addition of hydrogen influences the stereospecificity of the isospecific sites.[38] However, it is not clear how this might happen without an attendant loss in molecular weight (PP2-HI, M_n = 171 000; PP1-HI, M_n = 193 000).

An alternative interpretation of the fractionation results is that these unbridged catalysts in the presence of MAO lead to more than one type of catalyst site and that the isospecific sites are relatively insensitive to hydrogen. This latter interpretation is supported by the heterogeneous composition of the raw polymers, their broad molecular weight distributions ($2.7 < M_w/M_n < 3.2$), and the broad melting transitions.

The mechanism we have proposed involves at least two active catalytic species that interconvert on the time scale of a polymer chain lifetime.[18,19] This type of kinetic mechanism would be expected to generate a distribution of isotactic and atactic block lengths and thus some compositional heterogeneity.[35] In addition, this kinetic model predicts an increase in isotacticity with increasing monomer concentration. As seen in a comparison between PP3 and PP1, an increase in monomer concentration leads to an increase in the average isotactic pentad content of the polymer (PP3, [mmmm] = 0.17; PP1, [mmmm] = 0.32), a corresponding decrease in the ether-soluble weight fraction and the appearance of a heptane-insoluble fraction. This behavior is difficult to rationalize solely on the basis of a mixture of catalysts that do not interconvert at a rate competitive with monomer enchainment. Nevertheless, the observation of a high molecular weight heptane-insoluble fraction in both PP1 and PP2 provides strong indications that there is at least one catalyst site capable of producing a highly stereoregular polypropylene and that this site appears relatively insensitive to the presence of hydrogen. Thus, it is possible that the activation of unbridged 2-arylindene catalysts with MAO generates a mixture of active catalysts that have some distribution of rates of interconversion between the isospecific and aspecific forms. Further studies are underway to address whether the nature of the cocatalyst can influence the behavior of these unbridged catalysts.[39]

For the thermal studies, the DSC scans of the fractions also showed broad melting transitions and large standard deviations for ΔH_f. Upon aging of the fractions, double melting peaks and increased enthalpies of fusion were observed as in the whole polymer case. The ether-soluble fractions of all samples exhibit no thermal transition. For the other fractions, the lower the isotactic pentad content, the lower the crystallization/melting temperatures and enthalpies of crystallization/fusion. This can be explained by the close correlation between isotacticity and crystallinity.[36,40,41] X-ray diffraction patterns of the heptane-soluble and heptane-insoluble fractions indicated the coexistence of α and γ crystalline phases (Figures 3 and 4). The ether-soluble fractions, however, only showed an amorphous halo.

Conclusions

Polypropylenes obtained from unbridged 2-arylindene catalysts in the presence of MAO exhibit elastomeric properties. Microstructural characterizations of three elastomeric polypropylenes made with unbridged 2-phenylindene zirconocene catalysts revealed each is a heterogeneous mixture of stereoblock polypropylenes of different molecular weight and tacticity. Tacticity appears to be the primary factor in determining the fractionation behavior. The ether-soluble fractions of all three samples were amorphous while the heptane-soluble and heptane-insoluble fractions exhibited broad melting endotherms that suggest a broad distribution of crystallite sizes and stabilities in these samples. The α crystalline phase is dominant in the raw polymers; in both heptane-soluble and -insoluble fractions, some γ crystalline phase was also observed. The fractionation behavior and studies on the influence of added hydrogen on the properties of the resulting polypropylenes are consistent with a distribution of catalyst sites that interconvert between isospecific and aspecific forms during the course of the polymerization.

Experimental Section

Sample Preparation. Polypropylene samples characterized in this paper, PP1, PP2, and PP3, were synthesized at Amoco Chemical Co. Polymerization runs were conducted in a 2-gallon autoclave. The MAO cocatalyst (Akzo type 4A, dried under vacuum at 60 °C) (2 g/10 mL) and bis(2-phenylindenyl)-zirconium dichloride (0.04 g/10 mL) solutions were prepared in toluene and then mixed. The mixture was allowed to age for 30 min at room temperature prior to its injection into the reactor. A nitrogen purge was used for injection. Both PP1 and PP2 were synthesized from the bulk by using liquid propylene monomer. For sample PP2, hydrogen was added to the reactor to lower the molecular weight. PP3 was synthesized in hexane solution at 50 psig propylene. For all

three polymerizations, the reactor temperature was maintained at 20 °C prior to catalyst injection and at 23 °C during the reaction. After 2 h, the reaction mixture was pressurized into a solution of hexane and methanol to terminate the polymerization. Solvent and unreacted propylene monomer were removed, and the crude polymer was dried at 50 °C in vacuo. Yields for bulk and solution polymerizations under these conditions were approximately 130 and 30 g, respectively.

Purification. A 500 mL round-bottom flask was charged with xylene (300 mL) and 2,6-di-*tert*-butyl-4-methylphenol (BHT) (1 g). The crude polymer was dissolved at reflux in this solution under a nitrogen blanket. The hot polymer solution was filtered over Celite under vacuum and precipitated into acidified methanol (1% HCl) with vigorous stirring. The rubbery white precipitate was frozen in liquid nitrogen, ground in a blender, washed with acidified methanol (100 mL, 10% HCl), and dried overnight at 60 °C in vacuo.

Fractionation. The polymer samples were fractionated by successive extraction with boiling ether and heptane under a nitrogen blanket. A 500 mL round-bottom flask was charged with solvent (300 mL, w/ BHT) and attached to a Kumagawa extractor. The polymer (ca. 8 g) was packed into a thimble, layered with a plug of glass wool, and capped with filter paper (Whatman #1). The extractor was wrapped with aluminum foil and heated such that the flushing frequency of the extractor was ca. 4 min. The polymer samples were extracted for 24 h and then precipitated by pouring into acidified methanol (3000 mL, 1% HCl) with vigorous stirring. This process was repeated twice for each solvent and the thimble with contents was dried using an air flush at room temperature between solvent changes. The heptane-insoluble polymer remaining in the thimble was dried by aspiration at room temperature. The heptane-insoluble fraction was then redissolved in refluxing xylene (300 mL, 1 g BHT), hot filtered over glass wool with vacuum, and precipitated by pouring into acidified methanol (3000 mL, 1% HCl) with vigorous stirring. All of the precipitated samples were frozen using liquid nitrogen, ground in a blender, and washed with acidified methanol (150 mL, 10% HCl) before drying at 60 °C in vacuo.

IR. Infrared analysis was performed using a Perkin-Elmer 1600 series FT-infrared spectrometer. Polymer samples (0.02 g) were wrapped in aluminum foil and melt pressed at ca. 140 °C under 15 000 psig. The hot foil-wrapped films were removed from the press, quenched into liquid nitrogen, and peeled from the foil before warming. The films were allowed to stand overnight at room temperature prior to analysis. The films were scanned from 1600 to 450 cm^{-1} with a resolution of 2 cm^{-1}. Only four scans were required to obtain a sufficient level of signal-to-noise. The absorbance intensity of the peaks centered at 998 and 975 cm^{-1} were measured and baseline corrected. The IR index for each sample was calculated.

NMR. ^{13}C NMR spectra were obtained on a UNITY-INOVA 300 spectrometer equipped with a 10 mm probe operating at 75 MHz. The polymers were in a solution of 1,2-dideuteriotetrachloroethane (400 mg/3 mL) and the parameters used were as follows: temp, 100 °C; sweep width, 16 500 Hz; no. of repetitions, 1000; time domain, 64K; acquisition time, 1.001 s; pulse, 66.2°.

GPC. Molecular weights were obtained at Amoco Chemical Co. using high-temperature gel permeation chromatography (Waters 150C). Samples were run in 1,2,4-trichlorobenzene at 139 °C using two Polymer Laboratories PL GEL Mixed-B columns at a rate of 1 mL/min.

Thermal Analysis. Differential scanning calorimetry was performed on a Perkin-Elmer DSC 7 using indium as a calibration standard. Polymer samples (0.05 g) were wrapped in aluminum foil and melt pressed at ca. 140 °C using light pressure (<250 psig). The foil-wrapped films (ca. 1 mm thick) were removed from the press, quenched into liquid nitrogen, and peeled from the foil before warming. Disklike samples were punched from the cold films using a standard one-hole paper punch. These samples (ca. 0.015 g) were weighed and sealed into an aluminum DSC pan supplied by Perkin-Elmer. Samples were pretreated by heating from room temperature to 200 °C at 200 °C/min and held at 200 °C for 15 min. The crystallization temperature (T_c) and the enthalpy of crystallization (ΔH_c) were measured by cooling from +200 to −25 °C at 20 °C/min. The melting point (T_m) and the enthalpy of fusion (ΔH_f) were measured by cooling the pretreated samples from +200 to −50 °C at 200 °C/min and then scanning from −50 to +200 °C at 20 °C/min. To prepare aged samples, the samples were cooled from +200 to −50 °C at 20 °C/min and then heated to room temperature at 200 °C/min. The samples were allowed to stand at room temperature for 20 h prior to initiating the scans at −50 °C. All cycles were recorded three times to ensure reproducibility.

X-ray Analysis. X-ray powder diffraction patterns were obtained on a Rigaku diffractometer using a Cu Kα sealed beam source collimated with a Soller slit box containing a 5° opening angle and a system of diverging, receiving, and scattering slits with 1, 300, and 600 μm slit widths, respectively. A graphite monochromator was used. Polymer samples were wrapped in aluminum foil and melt pressed at ca. 140 °C using light pressure (<250 psig). The foil-wrapped films (ca. 1 mm thick) were removed from the press, quenched into liquid nitrogen, and peeled from the foil before warming. These films were wrapped in aluminum foil, placed in glass screw-cap vials, and flushed with nitrogen. The sealed vials were placed into a hot oil bath and allowed to equilibrate at 200 °C. After 30 min, the hot oil bath was shut off and the samples were allowed to cool slowly to room temperature, after which the samples were aged overnight prior to X-ray analysis. The powder diffraction patterns were measured over an angular range of 5−35° 2θ with an angular increment of 0.1° and a count time of 20 s. Analysis of the diffraction patterns was accomplished using the Shadow software package provided by Materials Data Inc. of Livermore, CA.

Mechanical Tests. Tensile tests and recovery tests were performed in the lab of Charles L. Myers at Amoco Chemical Co. with ASTM D-1708 dumbell specimens (0.9 in. gauge length) die cut from compression-molded sheets. The crosshead separation rate was 25.4 cm/min for the hysteresis test and 51 cm/min for the other tests. Tensile stress relaxation was measured as the decrease in stress over 5 min at 50% elongation (1.5 × original gauge). The tensile set after 300% elongation (4 × original gauge) was measured according to the method described by Collette et al., from benchmarks and within 1−2 min of recovery (immediate set). No hold time was imposed at extension; the crosshead direction was immediately reversed at 300% elongation. The 100% elongation hysteresis test was performed by elongating the specimen to 2 × original gauge length in three successive cycles of extension and recovery, with a 30 s hold at 100% elongation and a 60 s hold after crosshead recovery between cycles. In this hysteresis test, the set is measured as the elongation at which stress (or force) exceeds the baseline on the subsequent cycle. Stress relaxation is measured as the decrease in stress (or force) during the 30 s that the specimen is held at extension. Retained force is measured as the ratio of stress at 50% elongation during the second cycle recovery to the initial stress at 100% elongation during the same cycle.

Acknowledgment. We thank the NSF for financial support (CHE-9615699 and DMR-9528636). R.M.W. is a recipient of NSF's Alan T. Waterman Award, for which he is grateful. Dr. L. Bendig of Amoco Chemical Co. is gratefully acknowledged for providing us with the elastomeric polypropylene samples. We also thank Dr. J. Austin of Fiberweb Corp. for helpful discussions of mechanical property tests.

Supporting Information Available: Tables S1−S11 giving a complete listing of statistical analysis results (using Bernoullian, Enantiomorphic Site, and Concurrent Two Site Models) for samples PP1, PP2, PP3, and their fractions (11 pages). See any current masthead page for ordering and Internet access instructions.

References and Notes

(1) Natta, G.; Mazzanti, G.; Crespi, G.; Moraglio, G. *Chim. Ind. (Milan)* **1957**, *39*, 275−283.
(2) Natta, G. U.S. Patent 3,175,999, 1965.
(3) Natta, G. *J. Polym. Sci.* **1959**, *34*, 531−549.
(4) Brintzinger, H. H.; Fischer, D.; Mulhaupt, R.; Rieger, B.; Waymouth, R. M. *Angew. Chem., Int. Ed. Engl.* **1995**, *34*, 1143−1170.
(5) Collette, J. W.; Tullock, C. W. (Dupont) U.S. Patent 4,335,-225, 1982.
(6) Collette, J. W.; Tullock, C. W.; MacDonald, R. N.; Buck, W. H.; Su, A. C. L.; Harrell, J. R.; Mulhaupt, R.; Anderson, B. C. *Macromolecules* **1989**, *22*, 3851−3858.
(7) Collette, J. W.; Ovenall, D. W.; Buck, W. H.; Ferguson, R. C. *Macromolecules* **1989**, *22*, 3858−3866.
(8) Mallin, D. T.; Rausch, M. C.; Lin, Y. G.; Dong, S.; Chien, J. C. W. *J. Am. Chem. Soc.* **1990**, *112*, 2030−2031.
(9) Chien, J. C.; Llinas, G. H.; Raush, M. D.; Lin, G. Y.; Winter, H. H.; Atwood, J. L.; Bott, S. G. *J. Am. Chem. Soc.* **1991**, *113*, 8569−8570.
(10) Lin, Y. G.; Mallin, D. T.; Chien, J. C. W.; Winter, H. H. *Macromolecules* **1991**, *24*, 850−854.
(11) Llinas, G. H.; Dong, S.-H.; Mallin, D. T.; Rausch, M. D.; Lin, Y.-G.; Winter, H. H.; Chien, J. C. W. *Macromolecules* **1992**, *25*, 1242−1253.
(12) Babu, G. N.; Newmark, R. A.; Cheng, H. N.; Llinas, G. H.; Chien, J. C. W. *Macromolecules* **1992**, *25*, 7400−7402.
(13) Cheng, H. N.; Babu, G. N.; Newmark, R. A.; Chien, J. C. W. *Macromolecules* **1992**, *25*, 6980−6987.
(14) Llinas, G. H.; Day, R. O.; Rausch, M. D.; Chien, J. C. W. *Organometallics* **1993**, *12*, 1283−1288.
(15) Gauthier, W. J.; Collins, S. *Macromol. Symp.* **1995**, *98*, 223−231.
(16) Gauthier, W. J.; Corrigan, J. F.; Taylor, N. J.; Collins, S. *Macromolecules* **1995**, *28*, 3771−3778.
(17) (a) Gauthier, W. J.; Collins, S. *Macromolecules* **1995**, *28*, 3779−3786. (b) Bravakis, A. M.; Bailey, L. E.; Pigeon, M.; Collins, S. *Macromolecules* **1998**, *31*, 1000−1009.
(18) Coates, G.; Waymouth, R. M. *Science* **1995**, *267*, 217−219.
(19) Hauptman, E.; Waymouth, R. M.; Ziller, J. W. *J. Am. Chem. Soc.* **1995**, *117*, 11586−11587.
(20) Bruce, M. D.; Coates, G. W.; Hauptman, E.; Waymouth, R. M.; Ziller, J. W. *J. Am. Chem. Soc.* **1997**, *119*, 11174−11182.
(21) Kravchenko, R.; Masood, A.; Waymouth, R. M. *Organometallics* **1997**, *16*, 3635−3639.
(22) Maciejewski-Petoff, J. L.; Bruce, M. D.; Waymouth, R. M.; Masood, A.; Lal, T. K.; Quan, R. W.; Behrend, S. J. *Organometallics* **1997**, *16*, 5909−5916.
(23) The statistical analyses typically converge to two solutions. The solutions reported in Table 2 are those in which the isotacticity is highest at the enantiomorphic site (i.e. $\alpha > \sigma$).
(24) Luongo, J. P. *J. Appl. Polym. Sci.* **1960**, *3*, 302−309.
(25) Sundell, T.; Fageholm, H.; Crozier, H. *Polymer* **1996**, *37*, 3227−3231.
(26) Myers, C. L. Unpublished results.
(27) Gomez, M. A.; Tanaka, H.; Tonelli, A. E. *Polymer* **1987**, *28*, 2227−2232.
(28) Turner Jones, A.; Aizlewood, J. M.; Beckett, D. R. *Makrol. Chem.* **1964**, *75*,
(29) Thomann, R.; Wang, C.; Kressler, J.; Mulhaupt, R. *Macromolecules* **1996**, *29*, 8425−8434.
(30) Bruckner, S.; Meille, S. V. *Nature* **1989**, *340*, 455−457.
(31) Kissin, Y. V.; Rishina, L. A. *Eur. Polym. J.* **1976**, *12*, 757−759.
(32) Zambelli, A.; Locatelli, P.; Provasoli, A.; Ferro, D. R. *Macromolecules* **1980**, *13*, 267−270.
(33) Zhu, S.-N.; Yang, X.-Z.; Chûjô, R. *Polym. J.* **1983**, *15*, 859−868.
(34) Inoue, Y.; Itabashi, Y.; Chûjô, R.; Doi, Y. *Polymer* **1984**, *25*, 1640−1644.
(35) Coleman, B. D.; Fox, T. G. *J. Am. Chem. Soc.* **1963**, *85*, 1241−1244.
(36) Paukkeri, R.; Lehtinen, A. *Polymer* **1993**, *34*, 4075−4082.
(37) Busico, V.; Cipullo, R.; Chadwick, J. C. *Macromolecules* **1994**, *27*, 7538−43.
(38) One possibility is that hydrogen reacts preferentially at the isospecific site and thus influences the tacticity by selectively terminating the isospecific site. Further studies are underway to probe the influence of hydrogen on these catalyst systems.
(39) Polse, J.; Waymouth, R. M. Manuscript in preparation.
(40) Haftka, S.; Konnecke, K. *J. Macromol. Sci., Phys.* **1991**, *B30*, 319−324.
(41) Burfield, D. R.; Loi, P. S. T.; Doi, Y.; Mejzik, J. *J. Appl. Polym. Sci.* **1990**, *41*, 1095−1114.

MA9803990